IIETA International Information and Engineering Technology Association
Advancing the World of Information and Engineering

Mathematical Modelling of Engineering Problems
Vol. 13, No. 2, February, 2026, pp. 418-428
Journal homepage: http://iieta.org/journals/mmep

Integrated Limit Equilibrium and Finite Element Modelling of Slope Stability Under Hydro-Mechanical and Stratigraphic Controls

Enas Hisham Mohammed*, Omar Abdulwahhab Khalaf, Ekhlas N. Mohammed Alansari, Raghad I. Zidan, Bassma Abdul Nafaa Saeed

Building and Construction Techniques Engineering Department, Technical Engineering College, Northern Technical University, Mosul 41002, Iraq

Corresponding Author Email: enas.alhayali@ntu.edu.iq

https://doi.org/10.18280/mmep.130218

Received: 6 November 2025
Revised: 17 January 2026
Accepted: 30 January 2026
Available online: 15 March 2026

Keywords:
slope stability, Limit Equilibrium Method, Finite Element Method, hydro-mechanical effects, groundwater fluctuation, rainfall infiltration, soil stratification

ABSTRACT

Slope stability is a fundamental concern in geotechnical engineering and is strongly influenced by the interaction between soil mechanical properties and environmental loading conditions. In this study, a numerical modelling framework was developed to evaluate slope stability using both Limit Equilibrium Methods (LEMs) and the Finite Element Method (FEM). A systematic parametric analysis was conducted to assess the effects of key variables, including shear strength parameters, slope geometry, unit weight, external surcharge loading, groundwater level variation, rainfall infiltration, and soil stratification on the Factor of Safety (FOS). The results showed that increasing soil cohesion and internal friction angle significantly improves slope stability. In contrast, higher unit weight and steeper slope angles led to a noticeable reduction in FOS. Hydrological factors, particularly rainfall infiltration and rising groundwater levels, were found to substantially decrease slope stability due to increased pore water pressure and the reduction of effective stress. In addition, simulations of layered soil systems indicate that placing a stronger cohesive layer beneath a weaker soil layer significantly enhances overall stability compared with the inverse configuration. A comparative analysis between LEM and FEM results demonstrated good agreement in the predicted safety factors. However, FEM provided deeper insight into stress redistribution and potential failure mechanisms. The proposed modelling framework offers a reliable and efficient approach for slope stability assessment and supports informed geotechnical design under complex hydro-mechanical and stratigraphic conditions.

1. INTRODUCTION

Slope stability analysis is a critical aspect of geotechnical engineering. It directly influences the safety, economic feasibility, and long-term performance of civil engineering projects such as embankments, cut slopes, dams, and transportation infrastructure. The stability of slopes is commonly evaluated using the Factor of Safety (FOS), representing the ratio between resisting and driving forces acting along a potential failure surface [1]. Failure of natural or engineered slopes can lead to catastrophic consequences, including loss of life, and infrastructure damage. It may also result in significant economic losses. These risks highlight the necessity for reliable stability assessment methods [2-4].

A variety of analytical and numerical techniques have been developed to evaluate slope stability. Among the most widely used approaches are the Limit Equilibrium Methods (LEMs). These include the Bishop, Morgenstern–Price, Ordinary (Fellenius), and Janbu methods. These methods evaluate stability by satisfying equilibrium conditions along assumed slip surfaces [5-7]. In contrast, the Finite Element Method (FEM) evaluates slope behavior by simulating stress–strain relationships within the soil mass. It also captures progressive failure mechanisms. This approach provides a more realistic representation of soil response, particularly under complex loading and hydraulic conditions [8]. Both approaches have been widely applied in slope stability studies [9-11].

Slope stability depends on both internal and external factors. Internal factors are related to the inherent properties of soil and rock masses. These include geological conditions, stratigraphy, slope geometry, soil type and shear strength parameters [12-14]. External factors include rainfall infiltration, groundwater fluctuations, and applied surface loads. These factors act as triggering mechanisms that reduce soil shear strength and increase driving forces. As a result, slope failure may occur. In recent years, data-driven approaches have been explored. These include machine learning techniques. They have been used to predict slope FOS based on soil properties, providing tools for rapid assessment [15]. Rainfall is one of the most critical external factors affecting slope stability. Rainfall infiltration increases pore water pressure and reduces effective stress within the soil mass. This process weakens soil shear resistance [16-20]. Previous studies have shown that both rainfall intensity and duration play a key role in slope stability. Prolonged or intense rainfall events are often associated with landslide occurrence

[21, 22]. In addition, probabilistic and machine learning approaches have been applied to assess slope reliability under varying environmental conditions [23].

Slope stabilization measures are commonly to improve slope safety. These include modifying slope geometry, increasing soil strength, and controlling groundwater conditions [24-26]. However, their effectiveness depends on the interaction between soil properties, slope geometry, loading conditions, and hydraulic behavior. Recent studies have emphasized the importance of integrating numerical modeling with advanced analytical methods. This integration improves the understanding of slope behavior and enhances design practices [27, 28]. In Iraq, particularly in Mosul, slope instability has received increasing attention. This is due to urban expansion, infrastructure development, and changing climatic conditions. Previous studies have used numerical methods to evaluate slope stability under different scenarios [29, 30]. However, many of these studies consider a limited number of parameters or rely on a single analysis method. This limitation may not fully represent the combined mechanical and environmental effects.

This study addresses this limitation by presenting a comprehensive comparative analysis using both LEM and the FEM. It evaluates the influence of key parameters on the FOS. These parameters include soil strength, slope geometry, unit weight, external loading, groundwater level, rainfall infiltration, and soil layering. The study also aims to clarify the strengths and limitations of each method and to provide practical insights into their applicability under different engineering conditions. The findings are intended to support engineers in slope design and stability assessment.

2. METHODOLOGY

2.1 Slop stability analysis

Slope stability analysis is commonly performed using limit equilibrium and numerical approaches, which are based on force–moment equilibrium concepts and elastic–plastic continuum theory, respectively [31, 32]. Each approach has distinct advantages and limitations; therefore, combining both methods can provide a more reliable and comprehensive evaluation of slope behavior. The LEM remains the most established and widely applied technique in slope stability analysis. It evaluates slope safety by satisfying equilibrium conditions along an assumed potential failure surface. In this study, several classical LEM formulations are employed, including the Ordinary (Fellenius), Bishop, Janbu, and Morgenstern–Price methods [33, 34]. These methods differ in the treatment of inter-slice forces and equilibrium equations, leading to variations in the computed FOS. The application of multiple LEM techniques enables systematic comparison between methods and facilitates assessment of the sensitivity of stability results to the underlying assumptions of each formulation.

To complement the LEM analyses, the FEM is also adopted in this research. Unlike LEM, FEM does not require the prior definition of a failure surface; instead, it models the soil mass as a continuous medium and evaluates the stress–strain response under elastic–plastic conditions [35]. This capability makes FEM particularly effective for identifying critical failure zones, analyzing stress redistribution, and evaluating the study then investigates slope behavior under complex loading and hydraulic conditions. In the present study, FEM is used to verify the results obtained from LEM and to provide additional insight into deformation behavior and failure mechanisms. The FOS is adopted as the primary indicator of slope stability and is defined as the ratio between resisting and driving forces acting along a potential slip surface [36]. Slope stability analyses were carried out using the Geo-Studio software package developed in Canada. The geotechnical software SLOPE/W (SLOPE/W) module was employed to perform LEM-based analyses. The finite element program SIGMA/W (SIGMA/W) was used to conduct stress analysis within the soil mass based on FEM principles and to evaluate its influence on slope stability [37, 38].

Although newer versions of Geo-Studio are available, Geo-Studio 2012 was selected for this study due to its proven reliability, extensive validation in previous geotechnical research, and its ability to integrate LEM and FEM analyses within a unified modeling framework. The software also provides robust tools for analyzing both simple and complex slope configurations under a wide range of hydraulic and loading conditions. These capabilities are essential for long-term stability assessments and slow drawdown analyses [39]. By employing both LEM and FEM approaches, this study evaluates slope stability from both equilibrium-based and stress-controlled perspectives. This dual approach enhances the reliability and engineering relevance of the obtained results.

2.2 Materials properties of the slope

The material properties adopted for the slope stability analyses were derived from laboratory test results obtained from soil samples collected at the study area. These properties were selected to represent the actual in-situ conditions as realistically as possible and were applied consistently in both the LEM and FEM analyses. A summary of the physical and mechanical properties used in the numerical modeling is presented in Table 1, which serves as the main reference for the soil parameters adopted throughout this study.

Soil classification was carried out based on grain-size distribution and Atterberg limits tests in accordance with the Unified Soil Classification System (USCS). Although the soil contains a noticeable silt fraction, the measured plasticity characteristics indicate that it is most appropriately classified as high-plasticity clay (CH). This classification is therefore adopted consistently throughout the analysis to avoid any ambiguity between descriptive soil terminology and standardized classification systems.

The shear strength parameters, including cohesion and internal friction angle, were obtained from laboratory testing and subsequently used as key input parameters for the slope stability models. These parameters were systematically varied within engineering-reasonable ranges to evaluate their influence on the FOS, while maintaining consistency with the baseline values reported in Table 1. The unit weight values employed in the analyses correspond to the tested density conditions of the soil samples. Variations in unit weight implicitly reflect differences in moisture content and compaction state, both of which are known to exert a direct influence on slope stability behavior. Although changes in moisture content were not modeled explicitly, the selected ranges of unit weight provide a practical means of assessing their overall effect on slope stability.

All material properties summarized in Table 1 were directly

incorporated into the numerical models, ensuring transparency, repeatability, and a clear linkage between laboratory measurements and analytical results.

Table 1. Physical properties of the soil used in the slope stability analysis

Property	Value	Unit	Standard
Constitutive model	Mohr–Coulomb	–	–
Drainage condition	Drained	–	–
Soil condition	Saturated	–	–
Soil classification	CH	–	ASTM D2487
Dry unit weight (γ_d)	16.76	kN/m³	ASTM D698
Wet unit weight (γ_m)	18	kN/m³	ASTM D698
Internal friction angle (φ)	22	°	ASTM D3080
Cohesion (c)	25	kPa	ASTM D3080
Elastic modulus (E)	10,000	kPa	–
Poisson's ratio (ν)	0.35	–	–
Void ratio (e)	0.68	–	–
Permeability coefficient (k)	1×10^{-7}	m/s	ASTM D2434
Specific gravity	2.7	–	ASTM D854
Liquid limit (LL)	72	%	ASTM D4318
Plastic limit (PL)	36	%	ASTM D4318
Plasticity index (PI)	36	%	ASTM D4318

2.3 Slope properties and boundary conditions

The geometric configuration of the slope was defined based on actual field conditions observed at the study site in Mosul, Iraq. The slope has a total height of 14 m, a base length of 40 m, and a crest width of 12 m. This results in an initial slope angle of 29°, as illustrated in Figure 1(a). This geometry was selected to represent a typical natural slope in the study area and to serve as a baseline model for evaluating the influence of various geotechnical and environmental parameters.

Appropriate boundary conditions were applied to ensure numerical stability and to realistically simulate the mechanical behavior of the slope. The lateral boundaries of the model were constrained against horizontal displacement (x = 0) to prevent rigid body movement. The base of the slope was fixed against both horizontal and vertical displacements (x = y = 0). These boundary conditions are commonly adopted in slope stability analyses to represent a stable underlying foundation and to minimize boundary effects on the computed results.

An external surcharge load was applied at a distance of 2 m from the crest of the slope, as shown in Figure 1(b). This load simulates structural or construction-related loads frequently encountered in engineering practice. This configuration enabled the assessment of stress redistribution and its influence on slope stability under loaded conditions.

The slope geometry and boundary conditions presented in Figure 1 were applied consistently throughout all subsequent analyses in this study. This approach ensures comparability and coherence among the different parametric scenarios investigated, allowing for systematic evaluation of each factor.

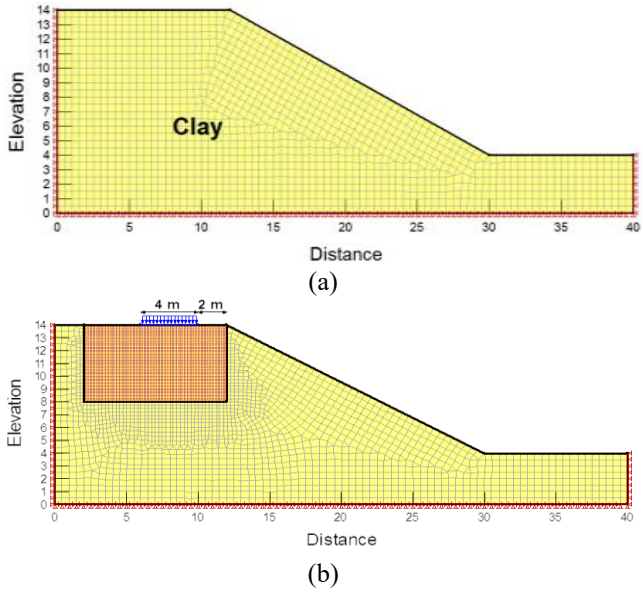

Figure 1. Geometry and boundary conditions of the modeled slope: (a) Geometry of the modeled slope and applied boundary conditions; (b) Location of the external surcharge load and corresponding boundary conditions

3. RESULTS AND DISCUSSION

3.1 Effect of shear strength coefficients

Slope stability analyses were conducted by varying the internal friction angle (22°, 25°, and 28°) while maintaining a constant soil cohesion of 25 kPa and a wet unit weight of 18 kN/m³. The slope angle was gradually increased from 29° to the critical value of 54.2°. Both LEM-Ordinary, Bishop, Janbu, and Morgenstern–Price- and the FEM were employed to evaluate the influence of shear strength parameters on slope stability. The results indicate that increasing the internal friction angle leads to a consistent increase in the FOS across all applied methods. This quasi-linear trend reflects the direct contribution of the friction angle to enhanced soil shear resistance along the potential failure surface, thereby improving resistance to sliding [40, 41]. Although all limit equilibrium approaches capture this behavior, variations in the predicted safety factors were observed due to differences in their underlying equilibrium assumptions. The Bishop and Morgenstern–Price methods generally exhibited higher sensitivity to changes in friction angle (Table 2).

Conversely, increasing the slope angle produces a pronounced destabilizing effect. As the slope inclination increases from 29° to 54.2°, the FOS decreases substantially, indicating that slope geometry plays a dominant role in controlling stability by amplifying the driving shear stresses acting along the potential slip surface.

The influence of soil cohesion was also examined by varying cohesion values while keeping other parameters constant. The FOS increased with higher cohesion values in both the limit equilibrium and finite element analyses (Table 3), which can be attributed to the enhanced shear strength provided by cohesive resistance [42, 43]. However, at the critical slope angle of 54.2°, the stabilizing effect of increased cohesion was significantly diminished, and the FOS decreased markedly. This observation confirms that under near-critical geometric conditions, slope geometry may override the

beneficial effects of improved soil strength and the associated shear resistance, which amplify the vertical loads acting on the soil mass.

Table 2. Safety factor values for a slope with a variable internal friction angle (ϕ) and slope angle (β)

γ_m (kPa)	**18**	**18**	**18**	**18**
c (kPa)	**25**	**25**	**25**	**25**
Slope angle (β°)	**54.2**	**48**	**39.8**	**29**
(Ø°)	**22**	**22**	**22**	**22**
Morgenstern–Price	1.030	1.173	1.444	2.097
Ordinary	0.659	1.096	1.359	2.013
Bishop	0.603	1.176	1.449	2.102
Janbu	0.526	1.098	1.342	1.970
Finite Element	1.027	1.186	1.459	2.103
(Ø°)	**25**	**25**	**25**	**25**
Morgenstern–Price	1.093	1.275	1.573	2.256
Ordinary	1.016	1.185	1.472	2.163
Bishop	1.095	1.279	1.579	2.261
Janbu	1.025	1.184	1.452	2.119
Finite Element	1.127	1.297	1.577	2.264
(Ø°)	**28**	**28**	**28**	**28**
Morgenstern–Price	1.200	1.389	1.712	2.420
Ordinary	1.108	1.283	1.595	2.305
Bishop	1.203	1.394	1.719	2.426
Janbu	1.113	1.279	1.571	2.257
Finite Element	1.231	1.411	1.707	2.431

Table 3. Safety factor values for a slope with a variable cohesion (C) of soil and slope angle (β)

γ_m (kPa)	**18**	**18**	**18**	**18**
C (kPa)	**16**	**16**	**16**	**16**
Slope angle (β°)	**54.2**	**48**	**39.8**	**29**
(Ø°)	**22**	**22**	**22**	**22**
Morgenstern–Price	0.864	1.088	1.210	1.704
Ordinary	0.688	0.789	1.122	1.621
Bishop	0.632	0.866	1.215	1.708
Janbu	0.526	0.556	1.107	1.590
Finite Element	0.886	1.012	1.218	1.714
C (kPa)	**25**	**25**	**25**	**25**
Morgenstern–Price	1.030	1.173	1.444	2.097
Ordinary	0.659	1.096	1.359	2.013
Bishop	0.603	1.176	1.449	2.102
Janbu	0.793	1.098	1.342	1.970
Finite Element	0.985	1.186	1.459	2.103
C (kPa)	**30**	**30**	**30**	**30**
Morgenstern–Price	1.070	1.224	1.556	2.305
Ordinary	1.012	1.164	1.481	2.211
Bishop	1.072	1.226	1.561	2.310
Janbu	1.023	1.167	1.462	2.160
Finite Element	1.027	1.280	1.580	2.309

3.2 Effect of dry weight unit

The dry unit weight is recognized as one of the key factors influencing the calculation of the FOS [44]. As shown in Table 4, for a slope characterized by an internal friction angle of 22°, a cohesion of 25 kPa, and dry unit weight values of 13, 14.9, 16.76, and 18.6 kN/m³. The results indicate that an increase in dry unit weight leads to a consistent reduction in the FOS across all applied methods.

Specifically, the Morgenstern–Price method indicates a decrease ranging from 12.4% to 17.3%. The Bishop method shows a reduction of approximately 12.3% to 19.8%. Similarly, the Janbu and Ordinary methods exhibit decreases of about 14.7%–17% and 14.2%–17.3%, respectively. The FEM also reflects a comparable decline in the FOS, ranging from 13.2% to 15.7%.

The reduction in the FOS is attributed to the increase in soil self-weight and the associated shear forces. These forces amplify the vertical loads acting on the soil mass, thereby increasing the driving forces relative to the available shear resistance.

In other words, as the dry unit weight increases, the mobilized shear strength becomes insufficient to counterbalance the enhanced gravitational forces. This leads to a progressive reduction in overall slope stability [45, 46].

Table 4. Safety factor values for a slope with a variable dry unit weight (γ_d) of soil and slope angle

(Ø°)	**22**				**22**			
C (kPa)	**25**				**25**			
Slope angle (β°)	**54.2**	**48**	**39.8**	**29**	**54.2**	**48**	**39.8**	**29**
γ_d (kN/m^3)	**14.9**	**14.9**	**14.9**	**14.9**	**13**	**13**	**13**	**13**
Morgenstern–Price	1.073	1.242	1.553	2.318	1.135	1.316	1.684	2.495
Ordinary	1.015	1.179	1.483	2.233	1.081	1.256	1.606	2.398
Bishop	1.074	1.244	1.558	2.324	1.136	1.317	1.688	2.500
Janbu	1.027	1.187	1.464	2.181	1.098	1.266	1.586	2.337
Finite Element	1.117	1.284	1.587	2.317	1.183	1.363	1.696	2.495
γ_d (kN/m^3)	**18.6**	**18.6**	**18.6**	**18.6**	**16.76**	**16.76**	**16.76**	**16.76**
Morgenstern–Price	0.994	1.141	1.404	2.064	1.032	1.207	1.489	2.176
Ordinary	0.928	1.070	1.328	1.982	0.968	1.131	1.407	2.093
Bishop	0.996	1.144	1.410	2.068	1.033	1.209	1.494	2.181
Janbu	0.937	1.071	1.310	1.940	0.975	1.135	1.389	2.047
Finite Element	1.027	1.186	1.459	2.103	1.054	1.220	1.506	2.181

3.3 Effects of the methods of analysis

Slope stability analyses were performed using the SLOPE/W software. Several (LEM)-namely Ordinary, Bishop, Janbu, and Morgenstern–Price were applied alongside the FEM to evaluate the FOS. The results show that the Bishop method consistently yields the highest FOS values. The Morgenstern–Price and Ordinary methods yielded slightly lower values, while the Janbu method produced the lowest FOS values, as illustrated in Figures 2(a)-(c).

The higher FOS values obtained using the Bishop method are attributed to its consideration of both moment equilibrium and inter-slice forces, as well as all vertical forces acting on the slices. This more comprehensive treatment of force equilibrium accounts for its slightly higher FOS, which deviates by 0.2% from the Morgenstern–Price method, 6.3% from the Janbu method and 4.2% from the Ordinary method.

The Morgenstern–Price method, which satisfies all equilibrium equations irrespective of force or moment assumptions, also produces relatively high FOS values, deviating by 6.1% from the Janbu method and 4% from the Ordinary method. In contrast, the Ordinary method yields lower FOS values because it does not fully satisfy horizontal and vertical force equilibrium and partially neglects lateral forces acting on the slices boundaries. Its FOS deviates by approximately 2.1% from that of the Janbu method, as it primarily considers slice weight and partial moment effects.

The Janbu method produces the lowest FOS values because it neglects moment equilibrium and shear forces, considering only inter-slice force equilibrium.

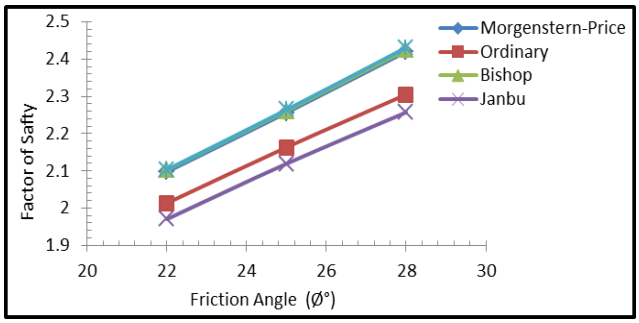

(a)

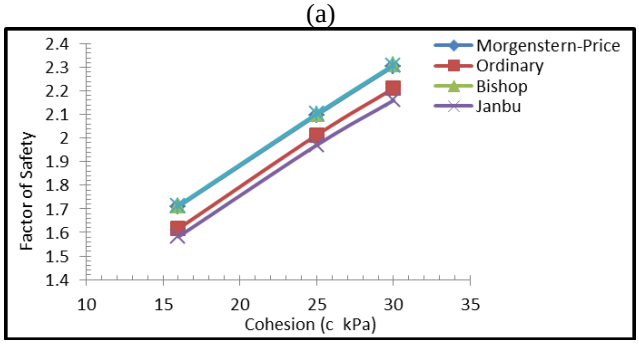

(b)

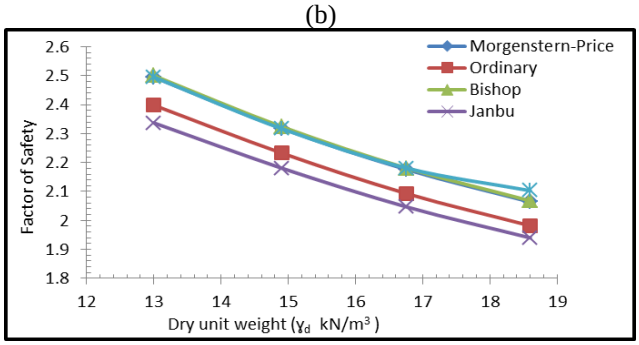

(c)

Figure 2. Relationship between the Factor of Safety (FOS): (a) Friction angle, (b) Cohesion, and (c) Dry unit weight using Limit Equilibrium Methods (LEM) and Finite Element Method (FEM)

In comparison with the LEM, the FEM provides a more realistic evaluation of slope stability. FEM identifies the critical sliding surface as the weakest zone within the soil mass, where shear resistance is minimal, and evaluates slope behavior based on stress–strain relationships under its governing assumptions. The deviations between the FOS values obtained from FEM and those from the LEMs are relatively small, amounting to 0.29% with respect to the Morgenstern–Price method, 0.05% relative to the Bishop method, 4.3% relative to the Ordinary method, and 6.3% relative to the Janbu method [47, 48].

3.4 Effect of slope angle (β)

The relationship between slope angle (β) and the FOS was evaluated using both LEM and the FEM, as illustrated in Figure 3. The slope angles considered in this study were 29°, 39.8°, 48°, and 54.2°, for slopes characterized by the properties summarized in the previous tables under normal conditions (i.e., without external loading). The results indicate that the FOS values obtained using the Bishop and Janbu methods are closely consistent, whereas the Morgenstern–Price, Ordinary, and FEM approaches produce comparable results. As the slope angle increases from 29° to 54.2°, the FOS decreases by approximately 53.4% for the Bishop and Janbu methods and by about 52.1% for the remaining methods. This decline in FOS follows a nonlinear trend, indicating that slope stability is highly sensitive to variations in slope angle [49, 50].

The reduction in the FOS with increasing slope angle is attributed to the increase in soil self-weight, which amplifies the vertical and shear components of the driving forces acting along the slope. As the slope becomes steeper, the available shear resistance becomes progressively smaller relative to the driving forces, thereby increasing the likelihood of sliding and potential failure [51, 52]. These findings highlight the critical role of slope geometry in controlling overall stability and emphasize that reducing slope inclination is an effective measure for enhancing slope safety.

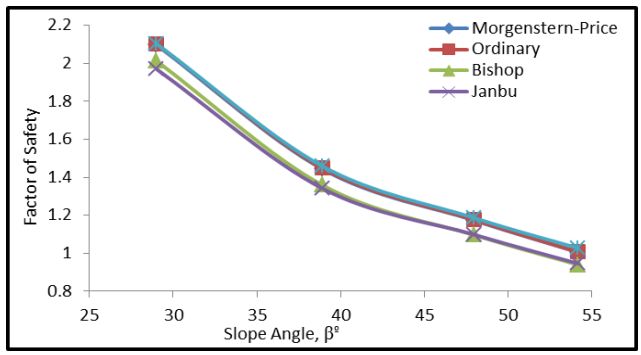

Figure 3. Relationship between the slope angle (β) and the Factor of Safety (FOS) using Limit Equilibrium Methods (LEM) and Finite Element Method (FEM)

3.5 Effect of external loads

External loads, such as those imposed by buildings or infrastructure, can be represented as applied forces defined by their magnitude and area of application, which determine the resulting stresses within the soil mass. In urban environments, slope stability may be significantly affected by human activities, including excavation, construction, and modifications to drainage conditions. Modern analytical approaches, such as advanced computational models and real-time monitoring techniques, provide effective tools for evaluating the influence of these factors on slope behavior [53].

Figure 1 shows the application of an external surcharge load of 250 kPa positioned 2 m from the slope crest. The impact of this load on the slope FOS is summarized in Figures 4–6. For slopes with internal friction angles between 22° to 28°, the application of the external surcharge load reduces the FOS decreases from 2.103, corresponding to an approximate 42% decrease (Figure 4). For slopes with cohesion values ranging from 16 and 30 kPa, the initial FOS of 1.714 decreases by approximately 38.9% under the same loading condition (Figure 5). Similarly, for slopes with dry unit weights from 13.6 to 18.6 kN/m³ and a slope angle of 29°, the external load causes a reduction in FOS of about 51.2%, as shown in Figure 6.

The reduction in the FOS under external loading primarily attributed to the increase in the vertical component of the sliding mass, which may exceed the available soil shear resistance. Additionally, the applied loads can elevate pore water pressure within the soil mass, further decreasing effective stress and shear resistance, thereby reducing the FOS [54]. Under unloaded conditions, slopes with an inclination of

54.2° are already close to failure; however, the application of external loads can trigger failure even at a reduced slope angle of 39.8°.

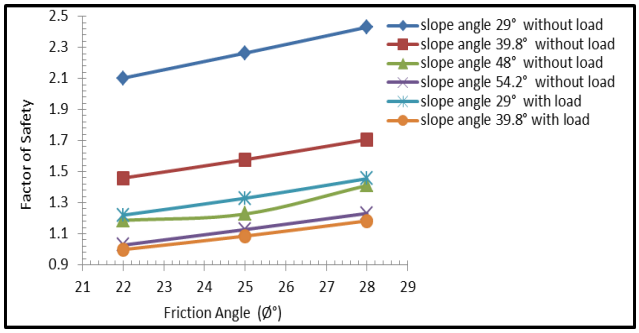

Figure 4. Relationship between the Factor of Safety (FOS) and the internal friction angle for a slope with and without external load using the Finite Element Method (FEM)

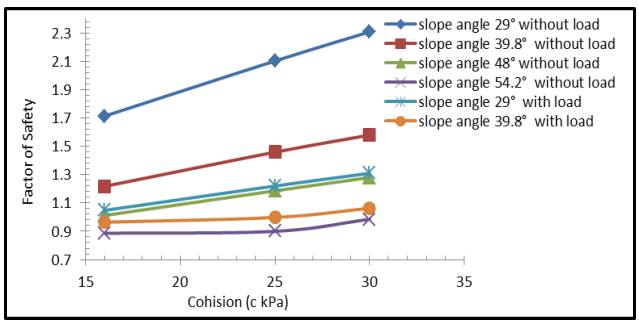

Figure 5. Relationship between the Factor of Safety (FOS) and cohesion for a slope with and without external load using the Finite Element Method (FEM)

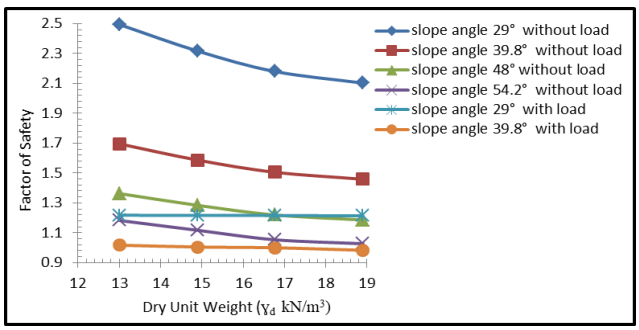

Figure 6. The connection between the Factor of Safety (FOS) and the dry unit weight for a slope with and without an external load using the Finite Element Method (FEM)

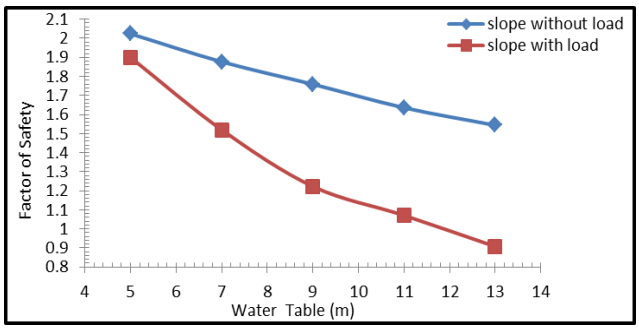

Figure 7. Effect of groundwater level on slope Factor of Safety (FOS) under unloaded and externally loaded conditions

3.6 Effect of changing water level within the slope

Water is a critical factor affecting the stability of earthen slopes, especially under seasonal variations such as rainfall infiltration, snowmelt, or proximity to surface and groundwater sources [55]. Figure 7 shows the variation in the FOS with increasing groundwater levels for slopes analyzed under both unloaded and externally loaded conditions. To assess this effect, groundwater levels measured from the slope base at 5, 7, 9, 11, and 13 m were considered. Two slope scenarios were analyzed: one without external loading and another subjected to an external surcharge load of 250 kPa. Identical soil properties were adopted for both cases ($\phi = 22°$, $\gamma_m = 12$ kN/m³, and C = 25 kPa).

Under dry conditions, the FOS was 2.103. As shown in Figure 7, a progressive reduction in the FOS was observed with increasing groundwater levels. Specifically, the FOS decreased by approximately 3.8% when the water table reached 5 m and by up to 26.6% when it rose to 13 m, indicating a trend toward unstable conditions. When the same groundwater levels were combined with an external surcharge load of 250 kPa, the destabilizing effect became more pronounced, leading to slope failure at a water level of 13 m.

The reduction in slope stability is primarily due to increased pore water pressure resulting from elevated groundwater levels. This increase decreases effective stress within the soil, thereby reducing its shear resistance. additionally, water infiltration weakens interparticle bonding by dissolving cementitious materials and surrounding soil particles, leading to reductions in both cohesion and internal friction. When an external surcharge load of 250 kPa is applied, these destabilizing effects are amplified. The combined increase in pore water pressure and the total weight of the soil mass enhances the driving forces relative to resisting forces, further reducing the FOS. Consequently, the simultaneous presence of elevated groundwater levels and external loading constitutes a critical condition for slope instability and potential failure [56, 57].

3.7 Effect of rainfall on the slope stability

Rainfall-induced landslides are among the most frequent and destructive natural hazards. Infiltrating rainwater penetrates the slope body rather than remaining on the surface, making rainfall a dominant triggering factor for slope failure [58, 59]. The influence of rainfall on slope stability was evaluated by considering two slope scenarios: one representing a natural slope without external loading and another subjected to an external surcharge of 250 kPa. Both scenarios employed identical soil properties, with an internal friction angle (ϕ) of 22°, a wet unit weight (γ_m) of 12 kN/m³, and cohesion (C) of 25 kPa. Rainfall intensities of 10, 30, and 50 mm/day were applied over periods ranging from 10 to 60 days, as depicted in Figure 8. This set up allowed for a systematic assessment of rainfall intensity and duration on slope stability under both unloaded and externally loaded conditions.

Under dry conditions, the initial FOS was 2.103. As rainfall intensity and duration increased, a progressive reduction in FOS was observed (Figure 9). At a low rainfall intensity of 10 mm/day, the FOS showed a moderate decrease during the early stages of infiltration before stabilizing, reflecting limited saturation depth and partial dissipation of matric suction. In contrast, higher rainfall intensities of 30 and 50 mm/day caused a rapid and substantial reduction in the FOS,

particularly during the first 10–30 days of infiltration. After this period, the FOS tended to stabilize as the soil approached near-saturated conditions, indicating that the rate of stability reduction decreases once the soil reaches high moisture content.

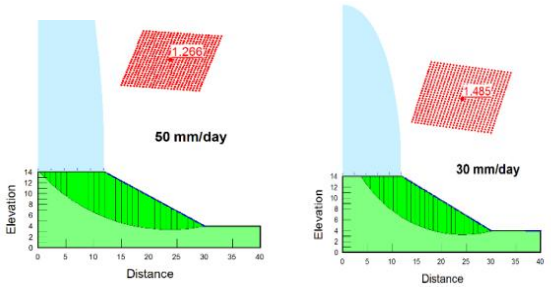

Figure 8. Effect of rainfall intensity on the stability of a natural slope under unloaded conditions

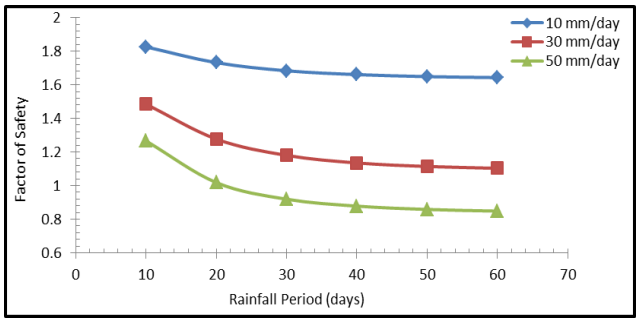

Figure 9. Variation of the Factor of Safety (FOS) with rainfall intensity and duration for a natural slope without external loading

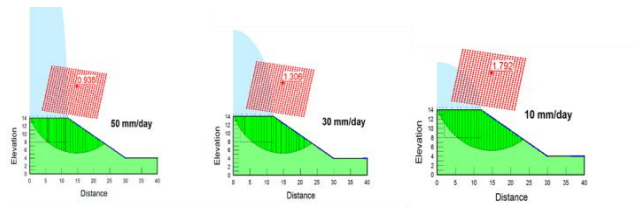

Figure 10. Effect of rainfall intensity and duration on the Factor of Safety (FOS) for a slope subjected to an external load of 250 kPa (Geostudio 2012 simulation)

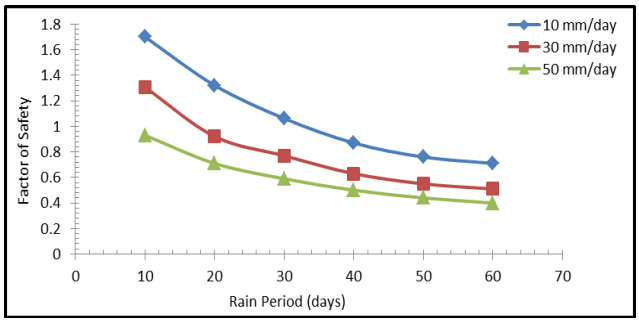

Figure 11. Variation of the Factor of Safety (FOS) with rainfall intensity and duration for a slope subjected to an external load of 250 kPa

When the same rainfall scenarios were applied to the slope subjected to an external surcharge load of 250 kPa, the destabilizing effect became considerably more pronounced. Figure 10 illustrates the loading condition, which amplified the reduction in the FOS shown in Figure 11. Even under low rainfall intensity 10 mm/day, the FOS experienced a noticeable decrease during the initial rainfall period. For higher rainfall intensities of 30 and 50 mm/day, the combined effect of prolonged infiltration and external loading caused a rapid reduction in the FOS, with values approaching critical or failure conditions within 10–40 days of rainfall.

The observed reduction in slope stability is primarily due to the hydromechanical interactions between rainfall infiltration and soil behavior. As rainfall continues, matric suction gradually diminishes and eventually vanishes when the soil becomes saturated. This leads to increased groundwater levels and pore water pressure, reducing effective stress and soil shear strength. The presence of an external load further these effect by increasing both the total driving forces and pore pressures within the slope, making soil mass susceptible to instability and potential failure [60-62].

3.8 Effect of two layers on the slope

Natural slopes frequently consist of multiple soil layers formed through long-term sedimentation, and such stratification can substantially influence slope stability behavior [63, 64]. In this study, both LEM and FEM were employed to systematically investigate the effect of soil layering on slope stability. The focus was placed on the mechanical role of layer sequencing rather than solely reporting numerical differences. Based on the soil properties summarized in Table 5, a second layer classified as silty soil (ML) was add to the original single-layer clay slope (CH). Using LEM, Figure 12 compares the stability of single-layer and two-layer slopes under varying slope angles. The results indicate that the introduction of the silty layer enhances the FOS, increasing values by approximately 63.3% to 70.6% relative to the single-layer slope, which exhibited values ranged from 1.97 to 2.102. As slope angle increases, the FOS values for different configurations tend to converge.

Table 5. Geotechnical properties of the second soil layer (ML) used as input parameters in the numerical slope stability analysis

Property	Soil Characteristics	Unit	Standard
The model used	Mohr-Coulomb		
Type of drainage	Drained		
Soil case	Saturated		
Soil type	ML		ASTM D 2487
Dry weight unit (γ_d)	15.8	kN/m^3	ASTM D 698
Wet weight unit (γ_m)	17.1	kN/m^3	
Internal friction angle (Ø)	14°		ASTM D 3080
Cohesion (C)	87	kN/m^2	ASTM D 3080
Modulus of elasticity (E)	20,000	kPa	
Poisson's ratio (υ)	0.4		

The FEM analysis, presented in Figure 13, corroborates the LEM findings, showing an improvement of approximately 68.9% in the FOS for the two-layer slope. To further evaluate the influence of layer arrangement, the lower silty layer was

replaced with a clayey layer characterized by significantly higher cohesion (c = 87 kPa). This modification resulted in a substantial increase in the FOS, as illustrated by the LEM results in Figure 14 and the FEM results in Figure 15. The observed improvement is primarily attributed to the enhanced cohesiveness and shear resistance of the clay layer, which reinforces the soil mass and effectively limits deformation and potential failure development.

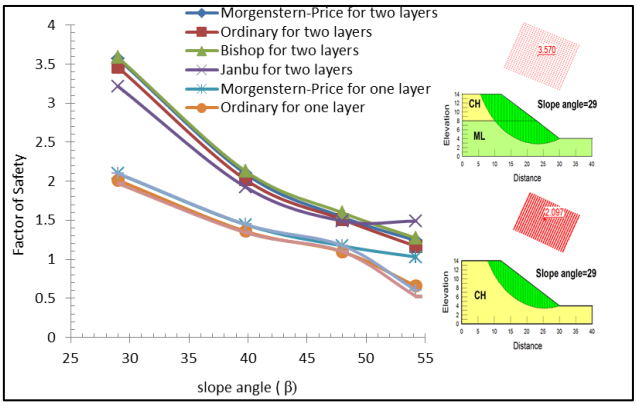

Figure 12. Comparison of the Factor of Safety (FOS) between single-layer and two-layer slope configurations under unloaded conditions using the Limit Equilibrium Method (LEM)

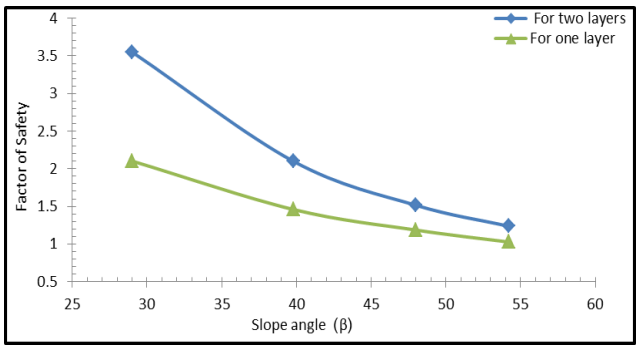

Figure 13. Comparison of the Factor of Safety (FOS) between single-layer and two-layer slope configurations under unloaded conditions using the Finite Element Method (FEM)

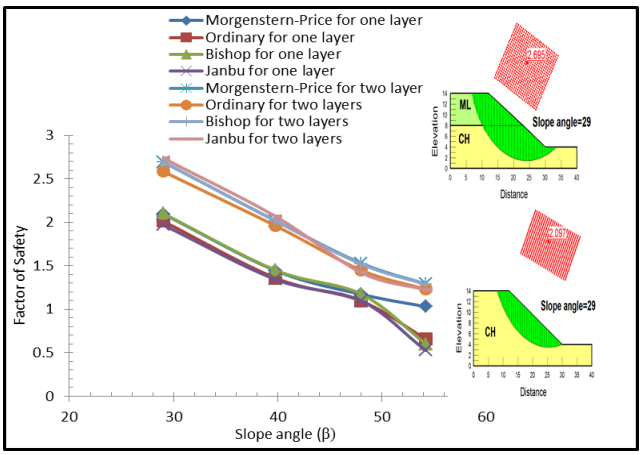

Figure 14. Comparison of the Factor of Safety (FOS) between single-layer and two-layer slope configurations under external loading using the Limit Equilibrium Method (LEM)

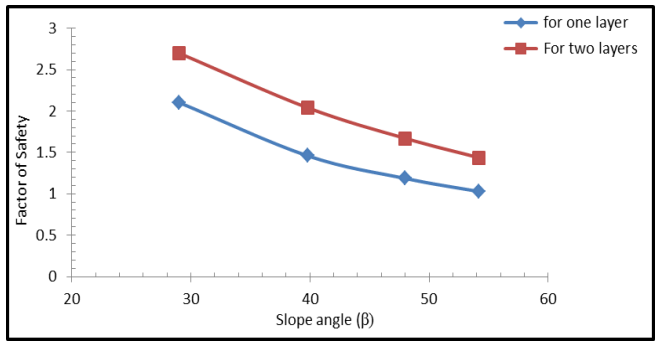

Figure 15. Comparison of the Factor of Safety (FOS) between single-layer and two-layer slope configurations under external loading using the Finite Element Method (FEM)

A key insight from these analyses is that slope stability is strongly governed by the vertical sequence of soil layers. Configurations in which a stronger, more cohesive clay layer underlies a weaker silty layer consistently yield higher FOS values than the reverse arrangement. This finding highlights the importance of accurate subsurface characterization in engineering practice, as the mechanical interaction between soil layers plays a decisive role in controlling slope performance and failure mechanisms.

4. CONCLUSIONS

(1). Shear strength parameters, specifically soil cohesion and internal friction angle, were as the primary determinants of slope stability. Higher values of these parameters enhance shear resistance along potential failure surfaces, directly improving overall stability. The observed near-linear relationship between the FOS and the internal friction angle emphasizes its dominant role in resisting sliding, particularly for moderately inclined slopes.

(2). An increase in soil dry unit weight consistently reduces slope stability. Higher unit weights amplify gravitational driving forces acting on the soil mass, which may exceed the mobilized shear resistance, especially for steep slopes. From an engineering perspective, this underscores the importance of controlling soil density and compaction during construction and slope modification activities to maintain safety margins.

(3). The choice of analytical method has a noticeable influence on the computed FOS. While LEM offer practical and computationally efficient estimates suitable for engineering design, the FEM provides a more realistic representation of stress redistribution and progressive failure mechanisms. The close agreement observed between FEM results and rigorous LEM formulations—such as the Bishop and Morgenstern–Price methods—confirms the reliability of these approaches when applied within appropriate assumptions. This finding highlights the importance of selecting suitable analytical techniques to achieve accurate stability assessments.

(4). Slope geometry has critical impact on slope stability. As the slope angle increases, the FOS decreases in a nonlinear manner due to the rapid growth of driving forces relative to resisting forces. This behavior emphasizes that geometric optimization, particularly slope flattening, remains one of the most effective and economic measures for improving slope stability in practical applications. The results underscore that

careful consideration of slope angles is essential during design and construction to prevent potential instability.

(5). External surcharge loads significantly reduce slope stability by increasing the driving forces acting on the soil mass. This increase leads to higher stress concentrations and may exceed the available shear resistance, particularly under unfavorable geometric or soil conditions. In addition, external loading can contribute to an increase in pore water pressure, further reducing effective stress and shear strength. These findings emphasize the importance of carefully evaluating.

(6). Hydrological factors, including rainfall intensity, rainfall duration, and rising groundwater levels, have a pronounced influence on slope stability. Water infiltration reduces matric suction and increases pore water pressure, leading to a decrease in effective stress and soil shear strength. As a result, the FOS declines, particularly under prolonged or high-intensity rainfall conditions. The combined effect of water infiltration and external loading further accelerates instability by simultaneously increasing driving forces.

(7). Soil stratification and layer sequencing play decisive role in controlling slope stability. Configurations in which a stronger and more cohesive layer underlies a weaker soil layer results in higher FOS values. This behavior is attributed to the enhanced shear resistant provided by the underlying layer. This layer limits deformation and restricts the development of potential failure surfaces. These findings highlight the importance of accurate subsurface characterization and appropriate layer arrangement in engineering design. The interaction between soil layers governs overall slope performance and influences the associated failure mechanisms.

5. RECOMMENDATIONS

Based on the outcomes of this study, future research is recommended to extend the present findings through three-dimensional slope stability analyses that better capture the interaction between soil layering, external loading, and complex slope geometries. The inclusion of dynamic loading conditions, such as seismic effects, is also suggested for slopes shown to be highly sensitive to changes in geometry and pore water pressure. In addition, advanced constitutive soil models should be employed to represent nonlinear and time-dependent behavior, particularly for clayey soils affected by rainfall infiltration and groundwater fluctuations. Finally, the performance of slope stabilization measures should be evaluated using coupled hydraulic–mechanical numerical approaches under the critical conditions identified in this study.

REFERENCES

[1] Li, L., Lin, H.J., Qiang, Y., Zhang, Y., Liang, S.Y., Hu, S.C., Xu, X.L., Ni, B. (2024). Stability analysis of rainfall-induced landslide considering air resistance delay effect and lateral seepage. Scientific Reports, 14: 8377. https://doi.org/10.1038/s41598-024-59121-4

[2] Beyabanaki, S.A.R. (2022). Impact of groundwater table fluctuation on stability of jointed rock slopes and landslides. Geotechnics, 2(2): 335-347. https://doi.org/10.3390/geotechnics2020015

[3] Tebbens, S.F. (2019). Landslide scaling: A review. Earth and Space Science, 7(1): e2019EA000662. https://doi.org/10.1029/2019EA000662

[4] Gatter, R., Cavalli, M., Crema, S., Bossi, G. (2018). Modelling the dynamics of a large rock landslide in the Dolomites (eastern Italian Alps) using multi-temporal DEMs. PeerJ. https://peerj.com/articles/5903/.

[5] Morgenstern, N.R., Price, V.E. (1965). The analysis of the stability of general slip surfaces. Geotechnique, 15(1): 79-93. https://doi.org/10.1680/geot.1965.15.1.79

[6] Spencer, E. (1967). A method of analysis of the stability of embankments assuming parallel inter-slice forces. Geotechnique, 17(1): 11-26. https://doi.org/10.1680/geot.1967.17.1.11

[7] Beyabanaki, S.A.R. (2021). Rock landslides induced by earthquakes: A study on influence of strength criterion on limit equilibrium stability analysis. International Journal of Engineering Research and Advanced Technology, 7(11): 18-29. https://doi.org/10.31695/IJERAT.2021.3744

[8] Li, A.J., Lyamin, A.V., Merifield, R.S. (2009). Seismic rock slope stability charts based on limit analysis methods. Computers and Geotechnics, 36(1-2): 135-148. https://doi.org/10.1016/j.compgeo.2008.01.004

[9] Gupta, A., Islam, M.A., Bin Alam, M.J. (2023). Numerical evaluation of slope stability based on temporal variation of hydraulic conductivity. E3S Web of Conferences, 382: 24003. https://doi.org/10.1051/e3sconf/202338224003

[10] Damiano, E., Olivares, L. (2010). The role of infiltration processes in steep slope stability of pyroclastic granular soils: Laboratory and numerical investigation. Natural Hazards, 52: 329-350. https://doi.org/10.1007/s11069-009-9374-3

[11] Islam, M.A., Islam, M.S., Elahi, T.E. (2020). Effectiveness of vetiver grass on stabilizing hill slopes: A numerical approach. In Geo-Congress 2020: Engineering, Monitoring, and Management of Geotechnical Infrastructure (GSP 316), pp. 106-115. https://doi.org/10.1061/9780784482797.011

[12] Sun, J.J., Xu, Ch., Feng, L.Y., Li, L., Zhang, X.W., Yang, W.T. (2024). The Yinshan mountains record over 10,000 landslides. Data, 9(2): 31. https://doi.org/10.3390/data9020031

[13] Askari, F.E., Farzaneh, O. (2008). Pore water pressures in three dimensional slope stability analysis. International Journal of Civil Engineering, 6(1): 10-23.

[14] Gunawan, H., Al-Huda, N., Sungkar, M., Yulianur, A., Setiawan, B. (2020). Slope stability analysis due to extreme precipitation. IOP Conference Series: Materials Science and Engineering, 796: 012044. https://doi.org/10.1088/1757-899X/796/1/012044

[15] Tun, S.H., Zeng, C., Jamil, F. (2025). Prediction of slope stability based on five machine learning techniques approaches: A comparative study. Multiscale and Multidisciplinary Modeling, Experiments and Design, 8: 224. https://doi.org/10.1007/s41939-025-00808-0

[16] Zeng, L., Shi, Z.N., Fu, H.Y., Bian, H.B. (2017). Influence of rainfall infiltration on distribution characteristics of slope transient saturated zone. China Journal of Highway and Transport, 30(1): 25-34. https://hal.science/hal-03247202v1.

[17] Qiu, X., Jiang, H.B., Ou, J., Fu, H.Y., Ma, J.Q. (2020). Numerical analysis of formation conditions and evolution characteristics of transient saturation zone of a

slope under rainfall conditions. Shuili Xuebao/Journal of Hydraulic Engineering, 51(12): 1525-1535. https://doi.org/10.13243/j.cnki.slxb.20200254
[18] Zeng, L., Bian, H.B., Shi, Z.N., He, Z.M. (2017). Forming condition of transient saturated zone and its distribution in residual slope under rainfall conditions. Journal of Central South University, 24: 1866-1880. https://doi.org/10.1007/s11771-017-3594-6
[19] Tang, D., Jiang, Z.M., Yuan, T., Li, Y. (2020). Stability analysis of soil slope subjected to perched water condition. KSCE Journal of Civil Engineering, 24(9): 2581-2590. https://doi.org/10.1007/s12205-020-1728-0
[20] Qiu, X., Li, J.H., Jiang, H.Q., Ou, J., Ma, J.Q. (2022). Evolution of the transient saturated zone and stability analysis of slopes under rainfall conditions. KSCE Journal of Civil Engineering, 26(4): 1618-1631. https://doi.org/10.1007/s12205-022-0733-x
[21] Kim, M.I., Lee, S.J. (2023). An analysis of landslide risk using the change in the volumetric water content gradient in the soil layer per unit time of effective cumulative rainfall. Water, 15(9): 1699. https://doi.org/10.3390/w15091699
[22] Xia, C.A., Zhang, J.Q., Wang, H., Jian, W.B. (2025). Global sensitivity analysis of slope stability considering effective rainfall with analytical solutions. Water, 17(2): 141. https://doi.org/10.3390/w17020141
[23] Raj, P., Roy, L.B. (2025). Assessing slope stability reliability through visual exploratory data analysis and machine learning in Kumaon region of Uttarakhand in India. SSRG International Journal of Civil Engineering, 12(1): 46-66. https://doi.org/10.14445/23488352/IJCE-V12I1P106
[24] Sharma, A.K., Ahirwar, Y. (2024). Importance of slope stabilization methods. International Advanced Research Journal in Science, Engineering and Technology, 11(3): 14-21. https://doi.org/10.17148/IARJSET.2024.11303
[25] Al-Hyasat, T., Ismeik, M., Hanandeh, S. (2025). Enhanced earth slope stability assessment using computational intelligence algorithms. Civil Engineering and Architecture, 13(3): 1597-1615. https://doi.org/10.13189/cea.2025.130312
[26] Omoregie, A.I., Ouahbi, T., Kan, F.K., Sirat, Q.A., Raheem, H.O., Rajasekar, A. (2025). Advancing slope stability and hydrological solutions through biocementation: A bibliometric review. Hydrology, 12(1): 14. https://doi.org/10.3390/hydrology12010014
[27] Yadav, D.K., Chattopadhyay, S., Tripathy, D.P., Mishra, P., Singh, P. (2025). Enhanced slope stability prediction using ensemble machine learning techniques. Scientific Reports, 15: 7302. https://doi.org/10.1038/s41598-025-90539-6
[28] Jing, Y.F., Li, Y.F., Chang, J., Liu, Z.B., Ni, Z.W., Wang, Q., Gao, D.F. (2025). Factor of safety prediction for slope stability using PCA and BPNN in Guangdong's H mining area. Scientific Reports, 15: 12804. https://doi.org/10.1038/s41598-025-95498-6
[29] Abbas, J.M. (2014). Slope stability analysis using numerical method. Journal of Applied Sciences, 14(9): 846-859. https://doi.org/10.3923/jas.2014.846.859
[30] Abbas, J.M. (2015). 2-D FEM for assessment of slope stability. Diyala Journal of Engineering Sciences, 8(2): 48-84. https://doi.org/10.24237/djes.2015.08207
[31] Kahatadeniya, K.S., Nanakorn, P., Neaupane, K.M. (2009). Determination of the critical failure surface for slope stability analysis using ant colony optimization. Journal of Engineering Geology, 108(1-2): 133-141. https://doi.org/10.1016/j.enggeo.2009.06.010
[32] Cheng, Y.M., Liu, H.T., Wei, W.B., Au, S.K. (2005). Location of critical three dimensional non-spherical failure surface by NURBS functions and ellipsoid with applications to highway slopes. Computers and Geotechnics, 32(6): 387-399. https://doi.org/10.1016/j.compgeo.2005.07.004
[33] Wei, W.B., Cheng, Y.M., Li, L. (2009). Three-dimensional slope failure analysis by the strength reduction and limit equilibrium methods. Computers and Geotechnics, 36(1-2): 70-80. https://doi.org/10.1016/j.compgeo.2008.03.003
[34] Duncan, J.M. (1996). State of the art: Limit equilibrium and finite element analysis of slopes. Journal of Geotechnical Engineering, 122(7): 577-596. https://doi.org/10.1061/(ASCE)0733-9410(1996)122:7(577)
[35] Wang, Z., Jiang, X. (2012). Computational accuracy impact factors of slope stability safety factor and finite element strength reduction method. Electronic Journal of Geotechnical Engineering (EJGE), 17: 3547-3558.
[36] Chmielewski, R., Bak, A., Muzolf, P., Sobczyk, K. (2024). Influence of calculation parameters on the slope stability of the historical rasos cemetery in Vilnius (Lithuania). Sustainability, 16(7): 2891. https://doi.org/10.3390/su16072891
[37] Rashed, A. (2014). A new prediction model for slope stability analysis. Alma Mater Studiorum Università di Bologna. Dottorato di ricerca in Ingegneria civile e ambientale, 26 Ciclo. https://doi.org/10.6092/unibo/amsdottorato/6628
[38] Gu, X., Song, L., Xia, X., Yu, C. (2024). Finite element method-peridynamics coupled analysis of slope stability affected by rainfall erosion. Water, 16(15): 2210. https://doi.org/10.3390/w16152210
[39] Abbas, J.M., Aljanabi, Q.A., Mutiny, Z.A. (2017). Slope stability analysis of an earth dam. Diyala Journal of Engineering Sciences, 10(1): 106-117. https://doi.org/10.24237/djes.2017.10110
[40] Zeng, J.X., Chen, T.J., Lu, C.J., Wang, T.H., Chen, Y.Q. (2024). New method and insight for stability analysis of compound slopes. Computers and Geotechnics, 165: 105874. https://doi.org/10.1016/j.compgeo.2023.105874
[41] Xu, B.B., Si, W. (2016). Influence of strength parameters of soil on the slope stability. MATEC Web of Conferences, 63: 02032. https://doi.org/10.1051/matecconf/20166302032
[42] Rotaru, A., Bejan, F., Almohamad, D. (2022). Sustainable slope stability analysis: A critical study on methods. Sustainability, 14(14): 8847. https://doi.org/10.3390/su14148847
[43] Fang, C., Shimizu, H., Nishiyama, T., Nishimura, S. (2020). Determination of residual strength of soils for slope stability analysis: State of the art review. Reviews in Agricultural Science, 8: 46-57. https://doi.org/10.7831/ras.8.0_46
[44] Raghuram, A.S.S., Negi, P.S., Basha, B.M., Moghal, A.A.B. (2024). Effect of sample size, dry unit weight, and hysteresis of expansive soil on SWCC and finite slope stability. International Journal of Geosynthetics and Ground Engineering, 10: 18. https://doi.org/10.1007/s40891-024-00531-9

[45] Gupta, P., Raghuwanshi, A.K., Bhargava, S. (2016). Effect of density and moisture on the slope stability of highway embankment. International Journal of Engineering Sciences & Research Technology, 5(7): 10-16. https://doi.org/10.5281/zenodo.56885
[46] Chen, Q., Yan, E., Huang, S.P., Chen, N., Xu, H.W., Chen, F.Y. (2025). Study on slope stability of paleo-clay strength degradation under soaking and wet–dry cycles. Water, 17(2): 172. https://doi.org/10.3390/w17020172
[47] Griffiths, D.V., Lane, P.A. (1999). Slope stability analysis by finite element. Geotechnique, 49(3): 387-403. https://doi.org/10.1680/geot.1999.49.3.387
[48] Sapuan, W.K.M., Velavan, Y., Mohamad, D. (2023). Comparison of slope stabilization analysis method by using changing geometry and soil nailing for slope failure. International Journal of Infrastructure Research and Management, 11(S): 76-83.
[49] Song, H.R., Huang, J.K., Zhang, Z.W., Jiang, Q.O., Liu, L.H., He, C.S., Zhou, Y. (2024). Analysis of water migration and spoil slope stability under the coupled effects of rainfall and root reinforcement based on the unsaturated soil theory. Forests, 15(4): 640. https://doi.org/10.3390/f15040640
[50] Habtemariam, B.G., Shirago, K.B., Dirate, D.D. (2022). Effects of soil properties and slope angle on deformation and stability of cut slopes. Advances in Civil Engineering, 2022(1): 4882095. https://doi.org/10.1155/2022/4882095
[51] Zhou, J., Qin, C. (2022). Stability analysis of unsaturated soil slopes under reservoir drawdown and rainfall conditions: Steady and transient state analysis. Computers and Geotechnics, 142(1): 104541. https://doi.org/10.1016/j.compgeo.2021.104541
[52] Satyanaga, A., Abishev, R., Sharipov, A., Wijaya, M., Hamdany, A.H., Moon, S.W., Kim, J. (2023). Effect of slope geometry on stability of slope in Almaty. E3S Web of Conferences, 382: 13005. https://doi.org/10.1051/e3sconf/202338213005
[53] Arriola, C., Aronés, E., Vega, V., Esenarro, D., Salas, G., Romero, A., Raymundo, V. (2025). Physical slope stability: Factors of safety under static and pseudo-static conditions. Infrastructures, 10(3): 53. https://doi.org/10.3390/infrastructures10030053
[54] Xue, J.W. (2025). Analysis of factors affecting slope stability based on the finite element strength reduction method. Academic Journal of Science and Technology, 17(2): 24-28. https://doi.org/10.54097/4z35nj47
[55] Jia, J., Mao, C.X., Tenorio, V.O. (2024). Slope stability considering multi-fissure seepage under rainfall conditions. Scientific Reports, 14: 11662. https://doi.org/10.1038/s41598-024-62387-3
[56] Taghizadeh, M.H., Vafaeiyan, M. (2014). Study on effect of water on stability or instability of the earth slopes. International Research Journal of Applied and Basic Science, 8(9): 1482-1487.
[57] Latief, R.H., Zainal, A.K. (2019). Effects of water table level on slope stability and construction cost of highway embankment. Engineering Journal, 23(5): 1-12. https://doi.org/10.4186/ej.2019.23.5.1
[58] Mia, A.J., Farazi, A.H., Mahmud, M.I. (2017). Factors affecting slope stability for triggering rainfall induced landslide at Chittagong City: A case study on 2007 and 2008 landslides. IOSR Journal of Mechanical and Civil Engineering (IOSR-JMCE), 14(4): 43-48. https://doi.org/10.9790/1684-1404044348
[59] Chen, R.H., Chen, H.P., Chen, K.S., Zhang, H.B. (2009). Simulation of a slope failure induced by rainfall infiltration. Environmental Geology, 58: 943-952. https://doi.org/10.1007/s00254-008-1574-8
[60] Gofar, N., Rahardjo, H. (2017). Saturated and unsaturated stability analysis of slope subjected to rainfall infiltration. MATEC Web of Conference, 101: 05004. https://doi.org/10.1051/matecconf/201710105004
[61] Wang, M.H., Li, L. (2025). Slope stability analysis considering degradation of soil properties induced by intermittent rainfall. Water, 17(6): 814. https://doi.org/10.3390/w17060814
[62] Wang, Y.J., Smith, J.V., Nazem, M. (2023). Effect of various rainfall conditions on the roadside stabilisation of slopes in Gippsland. International Journal of Civil Engineering, 21: 173-192. https://doi.org/10.1007/s40999-022-00752-x
[63] Sarkar, S., Chakraborty, M. (2021). Stability analysis for two-layered slopes by using the strength reduction method. International Journal of Geo-Engineering, 12: 24. https://doi.org/10.1186/s40703-021-00153-4
[64] Zhuang, Y.Z., Hu, X.Y., He, W.B., Shen, D.Y., Zhu, Y.J. (2024). Stability analysis of a rocky slope with a weak interbedded layer under rainfall infiltration conditions. Water, 16(4): 604. https://doi.org/10.3390/w16040604